Journal Pre-proof

Effect of Inhibition of Colony Stimulating Factor 1 Receptor on Choroidal Neovascularization in Mice

Petra Schwarzer, Despina Kokona, Andreas Ebneter, Martin S. Zinkernagel

PII: S0002-9440(19)30848-X

DOI: https://doi.org/10.1016/j.ajpath.2019.10.011

Reference: AJPA 3253

To appear in: *The American Journal of Pathology*

Received Date: 11 December 2018

Revised Date: 9 July 2019

Accepted Date: 21 October 2019

Please cite this article as: Schwarzer P, Kokona D, Ebneter A, Zinkernagel MS, Effect of Inhibition of Colony Stimulating Factor 1 Receptor on Choroidal Neovascularization in Mice, *The American Journal of Pathology* (2019), doi: https://doi.org/10.1016/j.ajpath.2019.10.011.

Effect of Inhibition of Colony Stimulating Factor 1 Receptor on Choroidal Neovascularization in Mice

Petra Schwarzer*, MD, Despina Kokona*, PhD, Andreas Ebneter, MD, PhD, Martin S. Zinkernagel, MD, PhD

Department of Ophthalmology and Department of Department of Clinical Research, Inselspital, Bern University Hospital, University of Bern, Switzerland

Short title: Effect of CSF-1R inhibition on CNV in Mice

Number of text pages: 34; Number of tables: 1; Number of figures: 4

Footnote: P.S. and D.K. contributed equally to this work.

Funding: Supported by Swiss RetinAward 2017 from the Swiss VitreoRetinal Group (SVRG) and Bayer AG to P.S.

Corresponding author:

Martin S. Zinkernagel MD, PhD

Dept. Ophthalmology, Inselspital, Universität Bern 3010 Bern, Switzerland, Tel: +41 (0) 31 632 95 65, FAX: +41 (0) 31 382 01 14

martin.zinkernagel@insel.ch

Disclosures: PLX5622 chow was provided by Plexxikon Inc., Berkeley, CA, under a Materials Transfer Agreement. The sponsor or funding organizations had no role in the design or conduct of the experiments. The authors alone are responsible for the content and writing of this letter. P.S. and D.K. received grant support from Bayer. A.E. received honoraria from

Bayer for lectures and non-financial support from Allergan and Novartis. M.S.Z. received financial support from Allergan, Bayer, Heidelberg Engineering, Novartis, and equity Novartis.

Abstract

Neovascular age-related macular degeneration is one of the leading causes of blindness. Microglia and macrophages play critical role in choroidal neovascularization (CNV) and may therefore be potential targets to modulate the disease course. This study evaluated the effect of the colony stimulating factor-1 receptor (CSF-1R) inhibitor PLX5622 on experimental laser-induced CNV. A 98% reduction of retinal microglia cells was observed in the retina one week after initiation of PLX5622 treatment, preventing accumulation of macrophages within the laser site and leading to a reduction of leukocytes within the choroid after CNV induction. Mice treated with PLX5622 had a significantly faster decrease of the CNV lesion size as revealed by *in vivo* imaging and immunohistochemistry from day 3 to day 14 compared to untreated mice. Several inflammatory modulators, such as CCL9, granulocyte-macrophage colony-stimulating factor, ssoluble tumor necrosis factor receptor-I, interleukin-1α, and matrix metallopeptidase-2 were elevated in the acute phase of the disease when microglia were ablated with PLX5622, whereas other cytokines (eg, interferon-γ, interleukin-4, and interleukin-10) were reduced. Our results suggest that CSF-1R inhibition may be a novel therapeutic target in patients with neovascular age-related macular degeneration.

Introduction

The main feature of choroidal neovascularization (CNV) is new abnormal blood vessels emerging from the choroid and growing through Bruch's membrane and sometimes the retinal pigment epithelium (RPE). CNV is observed during neovascular age-related macular degeneration (AMD) and can lead to vision loss in patients suffering from AMD.[1, 2] Although the particular pathogenesis of AMD remains unknown, there are several previous studies showing the involvement of the innate immune system in the development of the disease [3-5].

Microglia, residing in the retina, are dynamic surveillants of the extracellular environment,[6] located mainly in the ganglion cell layer, the inner nuclear layer, and the outer plexiform and nuclear layers. They can become reactive upon injury and acquire migration and proliferation capabilities.[7] Several studies have suggested that along with resident microglia, infiltrating macrophages may also play a prominent role in the pathogenesis of AMD.[8-11] In AMD, microglia/macrophages have been found in the sub-retinal space, where they are associated with drusen accumulation and CNV.[12] In experimental laser-induced CNV microglia/macrophages depletion, using clodronate liposomes, resulted in reduced CNV size [13, 14] and other studies have shown that the CNV area is significantly reduced in mice knocked out for the C-C chemokine receptor type 2 (CCR2), a crucial component mediating macrophage infiltration.[15] CCR2 as well as the CX3C chemokine receptor 1 (CX3CR1) are considered important factors for recruitment of macrophages to areas of inflammation and for the trafficking and the cellular migration of microglia into the sub-retinal space.[12] There is increasing evidence for their role in AMD development as lower expression of CX3CR1 has been observed in patients with AMD.[16]

The involvement of microglia/macrophages in CNV is further supported by studies showing that reduction of immune cells' reactivity by intravitreal injections of polysialic acid

leads to reduced vascular leakage in a laser-induced CNV mouse model.[17, 18] Moreover, loss of interferon-β and transforming growth factor beta (TGF-β) signaling in retinal microglia has been implicated in increased microglia reactivity and exacerbated CNV lesions in mice, [19, 20] supporting a role of microglia cytokine signaling in the course of CNV.

Microglia depletion has been proven useful for the investigation of their involvement in several central nervous system (CNS) disease paradigms[21, 22] and it has been recently shown that brain microglia can be effectively eliminated by colony stimulating factor-1 receptor (CSF-1R) inhibition.[23, 24] This was also observed in the retina, where microglia cells were eliminated by 92% to 97% in mice kept on a CSF-1R inhibitor–supplied diet for one week[25, 26], while immune cells in the spleen were not affected after one to three weeks of PLX5622 treatment.[27-29] However, PLX5622-dependent reduction of antigen presenting cells and Ly6C^{low} monocytes in the blood and the bone marrow have been reported.[29, 30] Cessation of CSF-1R inhibitor resulted in repopulation of retinal microglia from the remaining resident microglia pool in a CX3CR1 dependent manner.[31, 32] However, more recent studies using bone marrow chimera mice suggest that monocyte-derived macrophages repopulate the retina, following cessation of PLX5622 treatment, where they adopt a ramified microglia-like morphology.[33] Here, the CSF-1R inhibitor PLX5622 was used during the whole duration of the experiments to gain insight in the role of retinal microglia/macrophages on the course of experimental laser-induced CNV.

Materials and Methods

Animals

This study was approved by the local Animal Ethics Committee (Veterinärdienst des Kantons Bern: BE 136/16) and conformed to the ARVO Statement for the Use of Animals in

Ophthalmic and Vision Research. Female mice were used, based on the observation that female mice are more prone to CNV formation.[34] C57BL/6J mice (Charles River Laboratories, Sulzfeld, Germany) and MacGreen (B6N.Cg-Tg(Csf1r-EGFP)1Hume/J)[35] heterozygous female mice (6 to 8 weeks old) were employed.

Mice had *ad libitum* access to PLX5622-containing chow (1200 parts per million [ppm] formulated in AIN-76A standard rodent diet; Research Diets, Inc., New Brunswick, NJ) or AIN-76A standard rodent diet (control chow). Animals were housed, in groups of 2 to 5, under temperature and humidity-controlled conditions in individually ventilated cages with a 12-hour light/12-hour dark cycle. Before laser treatment or imaging, mice were anesthetized with 1 mg/kg medetomidine (Dormitor 1 mg/mL; Provet AG, Lyssach, Switzerland) and 80 mg/kg ketamine (Ketalar 50mg/mL; Parke-Davis, Zurich, Switzerland) as previously described.[25] . At the end of the intervention, medetomidine was antagonized by injection of 2.25 mg/kg atipamezol (Antisedan 5mg/mL; Provet AG). Before and one week after the initiation of the PLX5622 diet, as well as at days 3, 7, and 14 after laser treatment, mouse retinas were examined using confocal laser scanning ophthalmoscopy, fundus autofluorescence, and fluorescein angiography (Heidelberg Spectralis HRA 2; Heidelberg Engineering GmbH, Heidelberg, Germany). Groups of mice were euthanized with CO_2 inhalation at days 3 and 7 after laser treatment and their retinas and choroid-RPE complexes were prepared for fluorescence-based flow cytometry (FACS) or retina and choroid-RPE whole mounts and histology. All experiments were repeated at least once.

Laser-induced Choroidal Neovascularization

Mice were anesthetized and laser coagulation was performed using a 532-nm argon laser (Visulas 532s; Carl Zeiss Meditec AG, Oberkochen, Germany) with a slit-lamp adapter (Iridex Corporation, Mountain View, CA) mounted on a slit-lamp (BM900; Haag-Streit AG,

Koeniz, Switzerland). Pupil dilation was achieved with tropicamide 0.5%/phenylephrine 2.5% eyedrops (Hospital Pharmacy, Inselspital, Bern, Switzerland). Hydroxypropyl methylcellulose 20 mg/mL (Methocel 2%; OmniVision AG, Neuhausen, Switzerland) was applied on the eyes to keep them hydrated. A 2-mm fundus lens (Ocular Instruments, Inc., Bellevue, WA) was used for fundus visualization during the laser application. Three spots per eye were applied around the optic nerve, avoiding the large vessels (50µm size, 300mW intensity, 100ms duration) and both eyes were lasered per mouse. Rupture of Bruch`s membrane was indicated by bubble formation directly after laser application. Lesions with obvious hemorrhage were excluded from analysis. Bridging between laser spots was avoided by positioning the laser sites with sufficient distance.

Fundus Autofluorescence Imaging

Mice were anesthetized and their pupils were dilated as described above. To avoid drying of the cornea with resulting impairment of image quality, hydroxypropyl methylcellulose 20 mg/mL (Methocel 2%; OmniVision AG, Neuhausen, Switzerland) was applied on each eye. Retinal images were acquired using an ultra-widefield 102º lens (Heidelberg Engineering GmbH, Heidelberg, Germany), as described previously.[36] In MacGreen mice, GFP-positive cells (microglia/macrophages) could be visualized as hyperfluorescent spots in the autofluorescence images.

Fluorescein Angiography

After induction of anesthesia and pupil dilation (see above) 50 µL of 0.01% fluorescein [Faure; Novartis, Switzerland; in 1x phosphate buffered saline (PBS)] was administered subcutaneously and images were acquired using the HRA system angiography (Heidelberg Spectralis HRA 2; Heidelberg Engineering GmbH, Heidelberg, Germany) with a

noncontact ultra-widefield 102º lens (Heidelberg Engineering GmbH, Heidelberg, Germany). Images were taken during the first 90 seconds. CNV area was marked and measured using the caliper function in the Heidelberg software by two blinded assessors (DK and PS) (Heidelberg Engineering GmbH, Heidelberg, Germany).

Immunohistochemistry Studies

For immunohistochemical studies, mouse eyes were isolated for preparation of retinal and choroid-RPE whole mounts. Eyes were fixed in 4% paraformaldehyde solution (PFA, pH 7.4) for 10 minutes, the anterior segments were removed (cornea and lens), and the posterior segment was incubated for another 50 minutes in PFA. Retinas were mechanically detached from the choroid-RPE complex and both tissues were extensively washed in 1x PBS, 0.5% TritonX-100 (Sigma-Aldrich, St. Louis, MO) and processed according to Ebneter, Kokona [37]. Isolectin GS-IB4 from Griffonia simplicifolia (Alexa Fluor 647 conjugate; 1:100; Thermo Fisher Scientific, Waltham, MA), a rabbit polyclonal antibody against ionized calcium-binding adapter molecule 1 (Iba-1; 1:500; ; Wako Pure Chemical Industries Ltd., Osaka, Japan) and a chicken polyclonal antibody against GFP (1:300; Abcam, Cambridge, UK) were used for labeling of blood vessels and microglia/macrophages. The secondary antibodies goat anti-rabbit IgG H+L (Alexa Fluor 594 conjugate; 1:200; Thermo Fisher Scientific, Waltham, MA) was used for the visualization of Iba-1 staining and goat polyclonal antibody to chicken IgY H+L (FICH; 1:200; Abcam, Cambridge, UK) for visualization of GFP staining.

Another group of mice was euthanized at days 3 or 7 after CNV induction and their eyes were fixed in 4% PFA (pH 7.4) overnight at 4 °C. Eyes were routinely embedded in paraffin and 5 µm paraffin sections were cut running through the optic nerve head. The slides were de-paraffinized and blocked with 10% NGS for 30 min prior to incubation with a rabbit polyclonal antibody against Iba-1 (see above) overnight at 4 °C. The slides were washed in 1x

PBS and incubated with a secondary biotinylated goat anti-rabbit IgG antibody (1:250; Vector Laboratories, Burlingame, CA), for 30 min in room temperature, followed by three washes with 1x PBS and incubation with an HRP-streptavidin-conjugate (1:1000; Vector Laboratories, Burlingame, CA) for 60 min at room temperature. The signal was visualized using the NOVA red substrate kit (Vector Laboratories, Burlingame, CA) according to manufacturer's instructions.

Microscopy

For retinal or choroid-RPE whole mounts, microscopy was performed on equipment provided by the Microscopy Imaging Center (MIC), University of Bern, Switzerland. Retinal and choroid-RPE flat mounts were examined using an inverted Zeiss LSM 710 fluorescence confocal microscope (Carl Zeiss Meditec AG, Jena, Germany). Z-stacks of 100 to 110 µm with 5 µm intervals were obtained. Eye sections were examined under a fluorescence Nikon Eclipse 80i microscope (Nikon, Tokyo, Japan). CorelDraw X6 (Corel Corporation, Ottawa, ON, Canada) was used for figure preparation.

Flow cytometry

Retinas and choroid-RPE complexes from MacGreen mice were used for flow cytometry analysis at days 3 and 7 after the laser application. The eyes were collected in PBS (pH 7.4), the anterior segment was removed, the retina was mechanically detached from the choroid-RPE complex and both tissues were used for flow cytometry. Retinas or choroid-RPE of each individual mouse were analyzed as one sample. Tissues were processed according to Ebneter, Kokona [37]. Retinas were stained with fluorescent-labelled antibodies against CD45-APC/Cy7 (30-F11, 1:400), CD11b-APC (M1/70, 1:200), and MHC-II-Pacific blue (major histocompatibility complex class-II, AF6-120.1, 1:200). Choroid-RPE samples were stained

with fluorescent-labelled antibodies against CD11b-APC (M1/70, 1:200), CD11c-APC/Cy7 (N418, 1:200), Ly6G-PerCP/Cy5.5 (1A8, 1:200), Ly6C-Brilliant Violet 405 (HK1.4, 1:100), NK-1.1-PE/Dazzle 594 (PK146, 1:200), CD3-PE/Dazzle 594 (17A2, 1:200), and CD19-PE/Dazzle 594 (6D5, 1:200). Zombie Red Fixable Viability Kit (1:800; Biolegend, San Diego, CA) staining was used for detection of dead cells, according to manufacturer's instructions. Samples were incubated for 20 minutes with an Fc blocker (1:200; Biolegend, San Diego, CA) followed by incubation with the fluorescent-labelled antibodies for 20 more minutes at 4 °C in the dark. Each experiment was repeated at least once.

An LSR II Cytometer System with the BD FACSDiva software V4.1 (BD Biosciences, Allschwil, Switzerland) was used for data acquisition. The flow cytometry data were analyzed with the Flowjo Single Cell Analysis Software V10 (TreeStar, Ashland, OR). All antibodies were purchased from Biolegend (San Diego, CA).

Protein extraction

In total, 34 C57BL/6J mice were used for protein extraction and analysis of cytokine and chemokine levels. Control or PLX5622-fed mice were lasered as mentioned above one week after the initiation of the PLX5622 diet and proteins were extracted from the posterior part of the eyes at day 3 and 7 post CNV. Ten naïve mice were used as naïve controls and four eyecups were pooled as one sample. Briefly, the eyecups were homogenized in 200 µL of lysis buffer [1x lysis buffer provided with the kit, 1 mM Na_3VO_4, protease inhibitor cocktail (cOmplete ULTRA Tablets, EDTA-free; Roche, Basel, CH)] and homogenized using a Precellys 24 tissue homogenizer (Bertin Instruments, Montigny-le-Bretonneux, France). After centrifugation for 10 min at 13000 rpm at 4 °C, the supernatant was collected and Bradford assay was used for the determination of total protein content.

Mouse inflammation antibody array-membranes

Mouse inflammation antibody array-membranes (ab193660; Abcam, Cambridge, UK) were processed according to manufacturer's instructions. Briefly, the membranes were incubated for 2 hours in blocking buffer (provided with the kit) and incubated with 500 µg of total protein, overnight at 4 °C. Membranes were washed (wash buffer provided with the kit) and incubated with biotin-conjugated anti-cytokines/chemokines (provided with the kit) in blocking buffer, overnight at 4 °C, and incubated with 1x HRP-conjugated streptavidin (provided with the kit), for 2 hours at room temperature. Chemiluminescence was detected using detection buffers (provided with the kit) and a Fusion Pulse Imaging System (Witec AG, Luzern, Switzerland). Densitometry analysis was performed using the "Protein Array Analyzer" function of the ImageJ2 software (https://imagej.net/ImageJ2; last accessed December 11, 2018).[38] The signal was normalized between different membranes using the positive control spots. Spots with abnormally high background were excluded from the analysis. The experiment was repeated once.

Statistical Analysis

The sample size was estimated in the GPower 3.1 software[39] based on a power of 0.8 (80%) and a significance level of 0.05 (5%). The standardized difference (SMD) of each experimental group was estimated based on previous studies and pilot experiments. D`Agostino-Pearson omnibus test or Kolmogorov-Smirnov test were used to test the normal distribution of different data sets. Repeated measures one-way ANOVA was used for the analysis of the CNV course with or without PLX5622 treatment. To compare the CNV area between PLX5622-treated and non-treated mice, ordinary one-way ANOVA was used followed by Tukey's post hoc analysis. Statistically significant differences of the flow cytometry data were determined using one-way ANOVA followed by Tukey's post hoc

analysis for normally distributed data and Kruskal-Wallis test followed by Dunn`s multiple comparison test for the data that did not follow normal distribution. Kruskal-Wallis test followed by Dunn`s multiple comparison test was used for the comparison of the array membrane data. All data are expressed as mean ± standard deviation (SD).

P-values less than 0.05 were considered statistically significant. GraphPad Prism 5.0 software (GraphPad Software, Inc., San Diego, CA) was used for the statistical analysis.

Results

Effect of CSF-1R inhibition in the time course of laser-induced CNV

Inhibition of the CSF-1R with PLX5622 for 7 days prior to CNV induction (Fig. 1A) led to a striking reduction of GFP positive cells in the retinas of mice (Fig. 1B). Laser application resulted in comparable CNV areas between PLX5622 treated and untreated mice three days after the CNV induction (Fig. 1C). However, the area of CNV was decreased at later time points in the CNV group (Fig. 1C), whereas the presence of PLX5622 resulted in an accelerated involution of CNV area over time (Fig. 1C). The leakage area of CNVs on the fluorescein angiographs substantiated this finding (Fig. 1D; ***$P < 0.001$, repeated measures one way ANOVA with Tukey's post hoc analysis). Moreover, at day 14, there was a statistically significant decrease in CNV size of mice fed with PLX5622 compared to control-fed mice (***$P < 0.001$, ordinary one way ANOVA with Tukey's post hoc analysis).

In the choroid-RPE complex, CNV areas were identified using isolectin GS-IB4 staining (Fig. 2A). Iba-1 positive cells representing microglia/macrophages accumulated around the lesion sites in the choroid-RPE and retinal whole mounts of control mice (Fig. 2A). In the PLX5622 group, Iba-1 positive cells, most probably representing macrophages, were present in CNV areas of the choroid-RPE but were absent from the neurosensory retina (Fig. 2A). In the choroid-RPE as well as in the outer retina, Iba-1 positive cells' morphology

suggested a reactive phenotype, whereas in the inner retina most of the Iba-1 positive cells had a ramified morphology (Fig. 2B). Iba-1 positive cells were also detected in eye sections around the lasered area of CNV-subjected mice and their numbers were greatly reduced in the presence of PLX5622 (Fig. 2C). In the choroid-RPE complex of MacGreen CNV-subjected mice the majority of CSF-1R-GFP positive cells were co-localized with Iba-1, whereas a few cells (arrows) were Iba-1 negative (Fig. 2D).

Quantification of microglia/macrophages with flow cytometry

Flow cytometry was performed at days 3 and 7 post CNV in the retina of control and PLX5622-treated CNV-subjected mice (Fig. 3A). The cells were gated as shown in Supplementary Figure 1A. CNV induced accumulation of $CD45^{low}CD11b^{+}$ microglia and $CD45^{hi}CD11b^{+}$ macrophages[40] in the retina, whereas PLX5622 reduced their numbers (Fig. 3A). Quantification of different cell populations revealed that the number of microglia and macrophages was elevated 3 and 7 days post CNV (Fig. 3B; ***$P < 0.001$, ordinary one way ANOVA with Tukey's post hoc analysis). In mice fed with PLX5622 microglia cells were diminished by approximately 98.5% compared to control CNV mice at day 3 and day 7 post CNV (Fig. 3B; ***$P < 0.001$, ordinary one way ANOVA with Tukey's post hoc analysis). Similarly, PLX5622 led to a reduction of macrophages by 47.7% and 76.3%, respectively, compared to control at days 3 and 7 post CNV induction (Fig. 3B; ***$P < 0.001$, ordinary one way ANOVA with Tukey's post hoc analysis). No statistically significant difference was observed in CSF-1R expression in different cell types for different treatments and time points (Fig. 3C). Increased MHC-II expression in both microglia and macrophages was observed at day 3 post CNV (Fig. 3C; ***$P < 0.001$, Kruskal-Wallis test followed by Dunn`s multiple comparison test). In mice fed with PLX5622 MHC-II expression in microglia and macrophages was virtually absent (Fig. 3C).

Quantification of immune cell population in the choroid-RPE with flow cytometry

Flow cytometry was performed at days 3 and 7 post CNV in the choroid-RPE of control and PLX5622-treated mice. The cells were gated as shown in Supplementary Figure 1B. The number of $CD11c^+$ cells, the majority of which most probably represents dendritic cells[41], leukocytes ($CD11b^+CD11c^{neg}$)[42], and neutrophils ($CD11b^+Ly6G^+$)[41] were elevated in the choroid-RPE during the acute phase of CNV (Fig. 4A; $*P < 0.05$, $**P < 0,01$, $***P < 0.001$, ordinary one-way ANOVA with Tukey's post hoc analysis for $CD11c^+$ cells and leukocytes, Kruskal-Wallis test followed by Dunn`s multiple comparison test for neutrophils), whereas PLX5622 led to a reduction of $CD11c^+$ cells and leukocyte numbers below control (naïve) levels (Fig. 4A). Interestingly, although there was no difference between the naïve and the CNV-subjected tissues in the total number of $Ly6G^{neg}$ $Ly6C^{low/neg}$ $SSC\text{-}H^{low}$ cells, representing non-classical patrolling monocytes/macrophages[43], the presence of PLX5622 led to a reduction of these cell numbers below control (naïve) levels (Fig. 4B; $***P < 0.001$, ordinary one way ANOVA with Tukey's post hoc analysis). Classical inflammatory monocyte/macrophages ($Ly6G^{neg}$ $Ly6C^{hi}$)[43] on the other hand, were increased at day 3 after CNV and this was prevented by PLX5622 (Fig. 4B; $***P < 0.001$, ordinary one way ANOVA with Tukey's post hoc analysis). The expression of CSF-1R by patrolling and inflammatory monocytes, expressed as a percentage of $Ly6G^{neg}$ $Ly6C^{low/neg}$ $SSC\text{-}H^{low}$ and $Ly6G^{neg}$ $Ly6C^{hi}$ cells, respectively, was not altered between the different groups (Fig. 4C, respectively).

Cytokine levels during the course of CNV

The protein levels of several inflammatory modulators such as chemokines (CCL3, CCL9), growth factors (IGFBP-3, IGFBP-5, GM-CSF), members of the TNF superfamily (CD30L, sTNFRI), inflammatory cytokines (interferon-γ, IFN-γ; interleukin-1α, IL-1α; inteleukin-12 p70, IL-12 p70), anti-inflammatory cytokines (interleukin-13, IL-13), matrix metalloproteinases (MMP-2, MMP-3), Fc gamma receptors (Fc-gamma RIIB), and adhesion

molecules (VCAM-1) were elevated at the acute phase of the disease (Table 1) 3 days after laser application. During the later phase (day 7), most of the inflammatory modulators returned to control levels except for an elevation of the protein levels of bFGF, GM-CSF, and VCAM-1. In the presence of PLX5622, protein levels of several targets were elevated (Table 1), in agreement with previous studies,[44] suggesting that PLX5622 actions are not mediated by a general reduction of the overall inflammatory response.

Discussion

Accumulation of microglia/macrophages in the subretinal space of CNV lesions and expression of inflammatory cytokines have both been implicated in the formation of CNV.[10, 12, 45, 46] However, the role of microglia/macrophages in CNV development is not clear yet, since contradictory roles of these cells have been reported. Previous studies have shown that macrophage depletion can lead to a reduction of VEGF production and CNV lesion size in mice,[13, 14] whereas other studies reported that lack of the CCR2 receptor and its ligand CCL2 in mice leads to spontaneous CNV development after 9 months of age.[2] Moreover, microglia accumulation has been observed in AMD lesions in CCL2/CX3CR1 deficient mice but not in control mice,[47] whereas several additional studies reported that resident microglia actively contribute to CNV development.[12, 48, 49] Microglia/macrophage involvement in CNV is further supported by studies showing that reduction of microglia and macrophages reactivity by polysialic acid or translocator protein 18 kDa (TSPO) ligands leads to reduced neurodegeneration and less vascular leakage in a CNV mouse model.[17, 50, 51]

Here, we show that CSF-1R inhibition with PLX5622 leads to faster involution of CNV, as revealed by *in vivo* imaging and immunohistochemical studies in retinal and choroid-RPE whole mounts (Figure 1 and 2). PLX5622 efficiently depletes retinal microglia as early as one week of treatment (Figs. 1, 2, and 3). The flow cytometry data showed that

PLX5622 reduced the total number of $CD45^{hi}CD11b^{+}$ cells in the retina, most probably representing invading monocyte-derived macrophages and perivascular macrophages, and largely prevented MHC-II expression by microglia and $CD45^{hi}CD11b^{+}$ cells (Figure 3C). of the effect of PLX5622 was not observed on CSF-1R expression by microglia or macrophages (Fig. 3C). Recent studies by Paschalis et al suggested that ocular injury could trigger infiltration of peripheral monocytes into the retina, where they adopt a ramified morphology similar to resting microglia and express low levels of CSF-1R.[33, 52] However, this was not observed in the present study.

Flow cytometry analysis was also performed in the choroid-RPE complex of CNV subjected mice fed with control or PLX5622 chow. These data revealed increased numbers of $CD11c^{+}$ cells, leukocytes, and neutrophils after CNV (Fig. 4), which is in agreement with previous studies.[53, 54] $CD11c^{+}$ dendritic cells have been previously reported to play a role in CNV development. Specifically, they have been found to accumulate in the CNV lesions, peaking in numbers between day 2 and 4 after laser-induced CNV in mice.[54] Moreover, intravenous injection of dendritic cells leads to their accumulation into the CNV lesions where they are associated with increased CNV size.[54] Our data are consistent with these findings. Moreover, inhibition of the CSF-1R with PLX5622 did not only deplete retinal microglia but it also affected the number of $CD11c^{+}$ cells and leukocytes found in the choroid-RPE by reducing their numbers below naïve levels, while it did not have any effect on neutrophil numbers (Fig. 4A). Previous studies have shown that CSF-1R signaling is vital for dendritic cells differentiation, and dendritic cells are diminished in the spleen and peritoneum of CSF-1R deficient mice.[55] Moreover, CSF-1R depletion has been recently shown to negatively regulate the dendritic cell pool size in adult mice.[56]

Further analysis of leukocyte subsets showed an increase of inflammatory classical monocytes/macrophages ($Ly6G^{neg}/Ly6C^{hi}$) 3 days post CNV, which was prevented by

PLX5622. However, the population of patrolling non-classical monocytes/macrophages in the choroid-RPE, identified as $Ly6G^{neg}/Ly6C^{low/neg}/SSC\text{-}H^{low}$, was not affected by laser-induced CNV, but PLX5622 reduced their number below naïve levels, while the remaining cells were still positive for CSF-1R expression (Fig. 4B). This suggests that PLX5622 leads to a reduction of resident choroidal macrophage numbers and prevents the recruitment of $Ly6C^{hi}$ inflammatory monocytes/macrophages into the affected area. Indeed, by using neutralizing antibodies against CSF-1R or its ligand CSF-1, it has been previously shown that blocking of CSF-1R signaling can lead to depletion of $Ly6C^{neg}$ monocytes in the blood, while it only has modest effects in $Ly6C^{+}$ monocytes in the bone marrow.[57-59] Thus, the beneficial effects of PLX5622 may be attributed at least partially to the reduced numbers of peripheral immune cells, which along with retinal microglia could contribute to the extracellular matrix remodeling that trigger the formation of new blood vessels.

To further investigate the effect of PLX5622 in the course of CNV, a panel of cytokines/chemokines were analyzed in CNV-subjected mice fed with PLX5622 or normal food, using a semi-quantitative assay (the array membrane data are openly available in OSF|Data repository - Open Science Framework at https://osf.io; reference number: y5n7h). Elevated levels of several cytokines/chemokines were found in the CNV-subjected eyes, while some of them were elevated even more in the presence of PLX5622 (Table 1). Among the highest up-regulated cytokines were CX3CL1, MMP-2, bFGF, and VCAM-1, whereas others, such as IL-6, TNFα, and MCP-1 were not changed compared to naïve mice. CX3CL1 signaling is a key modulator of macrophage recruitment into the injured tissues[60, 61] and it has been shown to reduce microglial activation and subsequent neurotoxicity.[62, 63] MMP-2 on the other hand has been reported to play a prominent role in CNV formation, since reduced CNV is observed in mice deficient for MMP-2.[64-66] MMPs can proteolytically cleave several

chemokines, leading to their inactivation or the generation of antagonistic derivatives, which cannot promote chemotaxis.[67]

No differences were detected in the levels of vascular endothelial growth factor (VEGF) between the experimental groups 3 and 7 days after CNV induction. VEGF is considered the major pro-angiogenic factor in the inflamed retina,[68-70] and it has been suggested that interaction between VEGF and other pro-angiogenic factors, such as bFGF, is required for the angiogenic actions of VEGF.[71] Here, an up-regulation of bFGF was observed in the presence or absence of PLX5622, but no differences were observed in VEGF protein levels between naïve and CNV mice in the presence or absence of PLX5622. Most likely, these differences could be observed in earlier time points after the CNV induction.

In the presence of PLX5622, the pro-inflammatory IL-1α was also elevated at day 3 after CNV laser-induction and it was significantly reduced at day 7. Up-regulation of the adhesion molecule VCAM-1 was also observed in our study and this up-regulation was greater in the presence of PLX5622. VCAM-1 mediates the adhesion of monocyte-derived macrophages to vascular endothelial cells and increased protein levels of VCAM-1 have been reported in the retinal vasculature during CNV in mice.[11] However, increased infiltration of monocyte-derived macrophages into the injured retina was not observed in the presence of PLX5622.

Additionally, significantly elevated levels of sTNFRI were found during the disease course of CNV in the presence of PLX5622. After TNF-α binds to its membrane receptors, TNFRI and TNFRII, the receptors are cleaved to their soluble forms (sTNFRI/sTNFRII) by metalloproteinases.[72] The level of surface expression of TNFRI and its soluble form was found to be an important factor in regulating TNFα-mediated effects,[73, 74] and the receptor cleavage acts as an important mechanism for the suppression of TNF-α–mediated inflammation.[75] The levels of the anti-inflammatory cytokines IL-4 and IL-10 were also

elevated in the PLX5622 group, and this was accompanied by down-regulation of IFN-γ levels. Indeed, IL-10 has been previously reported to inhibit the production of IFN-γ[76] and to mediate a suppressive effect on CNV development.[77] In addition, IL-4 has been shown to antagonize IFN-γ–induced activities in macrophages.[78-80] The expression of insulin-like growth factor–binding proteins (IGFBP-3, IGFBP-5, and IGFBP-6) was also increased in the presence of PLX5622. IGFBPs bind with high activity to insulin growth factor (IGF) and thus limit the free form of IGF in the circulation, [84-86] thereby acting as angiogenesis suppressors.[87-89] In keeping with this IGF signaling has been proposed to play a role in diabetic retinopathy and retinal neovascularization where it has been shown to lead to increased VEGF levels.[81-83]

Because of complex cytokine interactions that may act antagonistically, the apparent increase of the inflammatory cytokines after PLX5622, which is in keeping with previously published studies[44], may ultimately lead to a more angiostatic/anti-angiogenic phenotype and thus inhibits CNV progression. In addition, it has been previously reported that CSF-1 can increase the release of VEGF from monocytes and CSF-1R inhibition can lead to lower levels of VEGF.[90, 91] Thus, blockade of the receptor may affect the angiogenesis mediated by CSF-1R–expressing cells. Moreover, physical contact between immune cells, such as perivascular macrophages, and endothelial cells may be required for the progression of CNV. *In vitro* studies have shown that direct contact between monocytes and endothelial cells can increase endothelial cell proliferation.[92] [49, 93] Hence, reduction of retinal microglia and attenuation of perivascular macrophages could result in decreased endothelial cell proliferation and therefore regression of CNV lesions.

Our data are in agreement with previous studies that have shown elevation of cytokine and chemokine levels in the retinas of CNV-subjected mice, as well as infiltration of monocyte-derived macrophages into the retina early during the course of CNV.[11, 94-96] Apart

from microglia and monocyte-derived macrophages, RPE cells and vascular endothelial cells are also known to produce cytokines during CNV in mice.[97] Moreover, activated Müller cells could also be a source of cytokines during CNV. Based on the PLX5622 depletion data, immune cells are likely not the main producers of cytokines during the course of our CNV model, yet they play an important role in CNV progression.

In summary, the present study highlights the important role of innate immunity in the course of CNV in mice. Inhibition of the CSF-1R has beneficial effects against CNV progression but whether these effects are mediated by depletion of microglia and/or macrophages in the retina, by patrolling monocytes in the choroid or by the prevention of leukocyte influx needs to be further investigated. Additionally, a more detailed analysis of the cytokine and chemokine levels after PLX5622 treatment could provide valuable data towards specific biological effects of PLX5622 in retinal pathology.

Acknowledgments

We thank the Department for BioMedical Research (DBMR) of the University of Bern for the facilities and scientific and technical assistance.

P.S. designed and performed the experiments, analyzed and interpreted the data, and revised the manuscript. D.K. designed and performed the experiments, analyzed and interpreted the data, and wrote and revised the manuscript. A.E. contributed to the study design and revised the manuscript. M.Z. conceived and designed the experiments, interpreted the data, wrote and revised the manuscript, and supervised the project. All authors read and approved the final manuscript.

References

[1] Friedman DS, O'Colmain BJ, Munoz B, Tomany SC, McCarty C, de Jong PT, Nemesure B, Mitchell P, Kempen J, Eye Diseases Prevalence Research G: Prevalence of age-related macular degeneration in the United States. Archives of ophthalmology 2004, 122:564-72.
[2] Ambati J, Ambati BK, Yoo SH, Ianchulev S, Adamis AP: Age-related macular degeneration: etiology, pathogenesis, and therapeutic strategies. Survey of ophthalmology 2003, 48:257-93.
[3] Shaw PX, Stiles T, Douglas C, Ho D, Fan W, Du H, Xiao X: Oxidative stress, innate immunity, and age-related macular degeneration. AIMS molecular science 2016, 3:196-221.
[4] Kaarniranta K, Salminen A: Age-related macular degeneration: activation of innate immunity system via pattern recognition receptors. Journal of molecular medicine 2009, 87:117-23.
[5] Coughlin B, Schnabolk G, Joseph K, Raikwar H, Kunchithapautham K, Johnson K, Moore K, Wang Y, Rohrer B: Connecting the innate and adaptive immune responses in mouse choroidal neovascularization via the anaphylatoxin C5a and gammadeltaT-cells. Scientific reports 2016, 6:23794.
[6] Lee JE, Liang KJ, Fariss RN, Wong WT: Ex vivo dynamic imaging of retinal microglia using time-lapse confocal microscopy. Investigative ophthalmology & visual science 2008, 49:4169-76.
[7] Hanisch UK, Kettenmann H: Microglia: active sensor and versatile effector cells in the normal and pathologic brain. Nature neuroscience 2007, 10:1387-94.
[8] Killingsworth MC, Sarks JP, Sarks SH: Macrophages related to Bruch's membrane in age-related macular degeneration. Eye 1990, 4 (Pt 4):613-21.
[9] Penfold P, Killingsworth M, Sarks S: An ultrastructural study of the role of leucocytes and fibroblasts in the breakdown of Bruch's membrane. Australian journal of ophthalmology 1984, 12:23-31.
[10] Yang Y, Liu F, Tang M, Yuan M, Hu A, Zhan Z, Li Z, Li J, Ding X, Lu L: Macrophage polarization in experimental and clinical choroidal neovascularization. Scientific reports 2016, 6:30933.
[11] Caicedo A, Espinosa-Heidmann DG, Pina Y, Hernandez EP, Cousins SW: Blood-derived macrophages infiltrate the retina and activate Muller glial cells under experimental choroidal neovascularization. Experimental eye research 2005, 81:38-47.
[12] Combadiere C, Feumi C, Raoul W, Keller N, Rodero M, Pezard A, Lavalette S, Houssier M, Jonet L, Picard E, Debre P, Sirinyan M, Deterre P, Ferroukhi T, Cohen SY, Chauvaud D, Jeanny JC, Chemtob S, Behar-Cohen F, Sennlaub F: CX3CR1-dependent subretinal microglia cell accumulation is associated with cardinal features of age-related macular degeneration. The Journal of clinical investigation 2007, 117:2920-8.
[13] Sakurai E, Anand A, Ambati BK, van Rooijen N, Ambati J: Macrophage depletion inhibits experimental choroidal neovascularization. Investigative ophthalmology & visual science 2003, 44:3578-85.
[14] Espinosa-Heidmann DG, Suner IJ, Hernandez EP, Monroy D, Csaky KG, Cousins SW: Macrophage depletion diminishes lesion size and severity in experimental choroidal neovascularization. Investigative ophthalmology & visual science 2003, 44:3586-92.
[15] Tsutsumi C, Sonoda KH, Egashira K, Qiao H, Hisatomi T, Nakao S, Ishibashi M, Charo IF, Sakamoto T, Murata T, Ishibashi T: The critical role of ocular-infiltrating macrophages in the development of choroidal neovascularization. Journal of leukocyte biology 2003, 74:25-32.
[16] Falk MK, Singh A, Faber C, Nissen MH, Hviid T, Sorensen TL: CX3CL1/CX3CR1 and CCL2/CCR2 chemokine/chemokine receptor complex in patients with AMD. PloS one 2014, 9:e112473.
[17] Karlstetter M, Kopatz J, Aslanidis A, Shahraz A, Caramoy A, Linnartz-Gerlach B, Lin Y, Luckoff A, Fauser S, Duker K, Claude J, Wang Y, Ackermann J, Schmidt T, Hornung V, Skerka C, Langmann T, Neumann H: Polysialic acid blocks mononuclear phagocyte

reactivity, inhibits complement activation, and protects from vascular damage in the retina. EMBO molecular medicine 2017, 9:154-66.
[18] Langmann T, Fauser S: [Polysialic Acid for Immunomodulation in an Animal Model for Wet Age-Related Macular Degeneration (AMD)]. Klinische Monatsblatter fur Augenheilkunde 2017, 234:657-61.
[19] Luckoff A, Caramoy A, Scholz R, Prinz M, Kalinke U, Langmann T: Interferon-beta signaling in retinal mononuclear phagocytes attenuates pathological neovascularization. EMBO molecular medicine 2016, 8:670-8.
[20] Ma W, Silverman SM, Zhao L, Villasmil R, Campos MM, Amaral J, Wong WT: Absence of TGFbeta signaling in retinal microglia induces retinal degeneration and exacerbates choroidal neovascularization. eLife 2019, 8.
[21] Spangenberg EE, Lee RJ, Najafi AR, Rice RA, Elmore MR, Blurton-Jones M, West BL, Green KN: Eliminating microglia in Alzheimer's mice prevents neuronal loss without modulating amyloid-beta pathology. Brain : a journal of neurology 2016, 139:1265-81.
[22] Szalay G, Martinecz B, Lenart N, Kornyei Z, Orsolits B, Judak L, Csaszar E, Fekete R, West BL, Katona G, Rozsa B, Denes A: Microglia protect against brain injury and their selective elimination dysregulates neuronal network activity after stroke. Nature communications 2016, 7:11499.
[23] Elmore MR, Najafi AR, Koike MA, Dagher NN, Spangenberg EE, Rice RA, Kitazawa M, Matusow B, Nguyen H, West BL, Green KN: Colony-stimulating factor 1 receptor signaling is necessary for microglia viability, unmasking a microglia progenitor cell in the adult brain. Neuron 2014, 82:380-97.
[24] Elmore MR, Lee RJ, West BL, Green KN: Characterizing newly repopulated microglia in the adult mouse: impacts on animal behavior, cell morphology, and neuroinflammation. PloS one 2015, 10:e0122912.
[25] Kokona D, Ebneter A, Escher P, Zinkernagel MS: Colony-stimulating factor 1 receptor inhibition prevents disruption of the blood-retina barrier during chronic inflammation. Journal of neuroinflammation 2018, 15:340.
[26] Ebneter A, Kokona D, Jovanovic J, Zinkernagel MS: Dramatic Effect of Oral CSF-1R Kinase Inhibitor on Retinal Microglia Revealed by In Vivo Scanning Laser Ophthalmoscopy. Translational vision science & technology 2017, 6:10.
[27] Bellver-Landete V, Bretheau F, Mailhot B, Vallieres N, Lessard M, Janelle ME, Vernoux N, Tremblay ME, Fuehrmann T, Shoichet MS, Lacroix S: Microglia are an essential component of the neuroprotective scar that forms after spinal cord injury. Nature communications 2019, 10:518.
[28] Wheeler DL, Sariol A, Meyerholz DK, Perlman S: Microglia are required for protection against lethal coronavirus encephalitis in mice. The Journal of clinical investigation 2018, 128:931-43.
[29] Funk KE, Klein RS: CSF1R antagonism limits local restimulation of antiviral CD8(+) T cells during viral encephalitis. Journal of neuroinflammation 2019, 16:22.
[30] Baraldi C, Sacchelli L, Dika E, Lambertini M, Misciali C, Bianchi T, Fanti PA: Safety profile of chronic leg ulcer biopsy: a monocentric retrospective series on 866 patients. Giornale italiano di dermatologia e venereologia : organo ufficiale, Societa italiana di dermatologia e sifilografia 2018.
[31] Zhang Y, Zhao L, Wang X, Ma W, Lazere A, Qian HH, Zhang J, Abu-Asab M, Fariss RN, Roger JE, Wong WT: Repopulating retinal microglia restore endogenous organization and function under CX3CL1-CX3CR1 regulation. Science advances 2018, 4:eaap8492.
[32] Huang Y, Xu Z, Xiong S, Qin G, Sun F, Yang J, Yuan TF, Zhao L, Wang K, Liang YX, Fu L, Wu T, So KF, Rao Y, Peng B: Dual extra-retinal origins of microglia in the model of retinal microglia repopulation. Cell discovery 2018, 4:9.
[33] Paschalis EI, Lei F, Zhou C, Kapoulea V, Dana R, Chodosh J, Vavvas DG, Dohlman CH: Permanent neuroglial remodeling of the retina following infiltration of CSF1R inhibition-resistant peripheral monocytes. Proceedings of the National Academy of Sciences of the United States of America 2018, 115:E11359-E68.

[34] Zhu Y, Lu Q, Shen J, Zhang L, Gao Y, Shen X, Xie B: Improvement and optimization of standards for a preclinical animal test model of laser induced choroidal neovascularization. PloS one 2014, 9:e94743.
[35] Sasmono RT, Oceandy D, Pollard JW, Tong W, Pavli P, Wainwright BJ, Ostrowski MC, Himes SR, Hume DA: A macrophage colony-stimulating factor receptor-green fluorescent protein transgene is expressed throughout the mononuclear phagocyte system of the mouse. Blood 2003, 101:1155-63.
[36] Kokona D, Schneider N, Giannakaki-Zimmermann H, Jovanovic J, Ebneter A, Zinkernagel M: Noninvasive Quantification of Retinal Microglia Using Widefield Autofluorescence Imaging. Investigative ophthalmology & visual science 2017, 58:2160-5.
[37] Ebneter A, Kokona D, Schneider N, Zinkernagel MS: Microglia Activation and Recruitment of Circulating Macrophages During Ischemic Experimental Branch Retinal Vein Occlusion. Investigative ophthalmology & visual science 2017, 58:944-53.
[38] Schneider CA, Rasband WS, Eliceiri KW: NIH Image to ImageJ: 25 years of image analysis. Nature methods 2012, 9:671-5.
[39] Faul F, Erdfelder E, Lang AG, Buchner A: G*Power 3: a flexible statistical power analysis program for the social, behavioral, and biomedical sciences. Behavior research methods 2007, 39:175-91.
[40] Ford AL, Goodsall AL, Hickey WF, Sedgwick JD: Normal adult ramified microglia separated from other central nervous system macrophages by flow cytometric sorting. Phenotypic differences defined and direct ex vivo antigen presentation to myelin basic protein-reactive CD4+ T cells compared. Journal of immunology 1995, 154:4309-21.
[41] Liyanage SE, Gardner PJ, Ribeiro J, Cristante E, Sampson RD, Luhmann UF, Ali RR, Bainbridge JW: Flow cytometric analysis of inflammatory and resident myeloid populations in mouse ocular inflammatory models. Experimental eye research 2016, 151:160-70.
[42] Patel BV, Tatham KC, Wilson MR, O'Dea KP, Takata M: In vivo compartmental analysis of leukocytes in mouse lungs. American journal of physiology Lung cellular and molecular physiology 2015, 309:L639-52.
[43] Geissmann F, Manz MG, Jung S, Sieweke MH, Merad M, Ley K: Development of monocytes, macrophages, and dendritic cells. Science 2010, 327:656-61.
[44] Paschalis EI, Lei F, Zhou C, Chen XN, Kapoulea V, Hui PC, Dana R, Chodosh J, Vavvas DG, Dohlman CH: Microglia Regulate Neuroglia Remodeling in Various Ocular and Retinal Injuries. Journal of immunology 2019, 202:539-49.
[45] Miao H, Tao Y, Li XX: Inflammatory cytokines in aqueous humor of patients with choroidal neovascularization. Molecular vision 2012, 18:574-80.
[46] Yamamoto Y, Miyazaki D, Sasaki S, Miyake K, Kaneda S, Ikeda Y, Baba T, Yamasaki A, Noguchi Y, Inoue Y: Associations of inflammatory cytokines with choroidal neovascularization in highly myopic eyes. Retina 2015, 35:344-50.
[47] Tuo J, Bojanowski CM, Zhou M, Shen D, Ross RJ, Rosenberg KI, Cameron DJ, Yin C, Kowalak JA, Zhuang Z, Zhang K, Chan CC: Murine ccl2/cx3cr1 deficiency results in retinal lesions mimicking human age-related macular degeneration. Investigative ophthalmology & visual science 2007, 48:3827-36.
[48] Ma W, Zhao L, Fontainhas AM, Fariss RN, Wong WT: Microglia in the mouse retina alter the structure and function of retinal pigmented epithelial cells: a potential cellular interaction relevant to AMD. PloS one 2009, 4:e7945.
[49] Rymo SF, Gerhardt H, Wolfhagen Sand F, Lang R, Uv A, Betsholtz C: A two-way communication between microglial cells and angiogenic sprouts regulates angiogenesis in aortic ring cultures. PloS one 2011, 6:e15846.
[50] Scholz R, Caramoy A, Bhuckory MB, Rashid K, Chen M, Xu H, Grimm C, Langmann T: Targeting translocator protein (18 kDa) (TSPO) dampens pro-inflammatory microglia reactivity in the retina and protects from degeneration. Journal of neuroinflammation 2015, 12:201.
[51] Rashid K, Wolf A, Langmann T: Microglia Activation and Immunomodulatory Therapies for Retinal Degenerations. Frontiers in cellular neuroscience 2018, 12:176.

[52] Paschalis EI, Lei F, Zhou C, Kapoulea V, Thanos A, Dana R, Vavvas DG, Chodosh J, Dohlman CH: The Role of Microglia and Peripheral Monocytes in Retinal Damage after Corneal Chemical Injury. The American journal of pathology 2018, 188:1580-96.
[53] Lavalette S, Raoul W, Houssier M, Camelo S, Levy O, Calippe B, Jonet L, Behar-Cohen F, Chemtob S, Guillonneau X, Combadiere C, Sennlaub F: Interleukin-1beta inhibition prevents choroidal neovascularization and does not exacerbate photoreceptor degeneration. The American journal of pathology 2011, 178:2416-23.
[54] Nakai K, Fainaru O, Bazinet L, Pakneshan P, Benny O, Pravda E, Folkman J, D'Amato RJ: Dendritic cells augment choroidal neovascularization. Investigative ophthalmology & visual science 2008, 49:3666-70.
[55] MacDonald KP, Rowe V, Bofinger HM, Thomas R, Sasmono T, Hume DA, Hill GR: The colony-stimulating factor 1 receptor is expressed on dendritic cells during differentiation and regulates their expansion. Journal of immunology 2005, 175:1399-405.
[56] Percin GI, Eitler J, Kranz A, Fu J, Pollard JW, Naumann R, Waskow C: CSF1R regulates the dendritic cell pool size in adult mice via embryo-derived tissue-resident macrophages. Nature communications 2018, 9:5279.
[57] Hashimoto D, Chow A, Greter M, Saenger Y, Kwan WH, Leboeuf M, Ginhoux F, Ochando JC, Kunisaki Y, van Rooijen N, Liu C, Teshima T, Heeger PS, Stanley ER, Frenette PS, Merad M: Pretransplant CSF-1 therapy expands recipient macrophages and ameliorates GVHD after allogeneic hematopoietic cell transplantation. The Journal of experimental medicine 2011, 208:1069-82.
[58] Lenzo JC, Turner AL, Cook AD, Vlahos R, Anderson GP, Reynolds EC, Hamilton JA: Control of macrophage lineage populations by CSF-1 receptor and GM-CSF in homeostasis and inflammation. Immunology and cell biology 2012, 90:429-40.
[59] Louis C, Cook AD, Lacey D, Fleetwood AJ, Vlahos R, Anderson GP, Hamilton JA: Specific Contributions of CSF-1 and GM-CSF to the Dynamics of the Mononuclear Phagocyte System. Journal of immunology 2015, 195:134-44.
[60] Combadiere C, Potteaux S, Rodero M, Simon T, Pezard A, Esposito B, Merval R, Proudfoot A, Tedgui A, Mallat Z: Combined inhibition of CCL2, CX3CR1, and CCR5 abrogates Ly6C(hi) and Ly6C(lo) monocytosis and almost abolishes atherosclerosis in hypercholesterolemic mice. Circulation 2008, 117:1649-57.
[61] Combadiere C, Potteaux S, Gao JL, Esposito B, Casanova S, Lee EJ, Debre P, Tedgui A, Murphy PM, Mallat Z: Decreased atherosclerotic lesion formation in CX3CR1/apolipoprotein E double knockout mice. Circulation 2003, 107:1009-16.
[62] Pabon MM, Bachstetter AD, Hudson CE, Gemma C, Bickford PC: CX3CL1 reduces neurotoxicity and microglial activation in a rat model of Parkinson's disease. Journal of neuroinflammation 2011, 8:9.
[63] Mizuno T, Kawanokuchi J, Numata K, Suzumura A: Production and neuroprotective functions of fractalkine in the central nervous system. Brain research 2003, 979:65-70.
[64] Berglin L, Sarman S, van der Ploeg I, Steen B, Ming Y, Itohara S, Seregard S, Kvanta A: Reduced choroidal neovascular membrane formation in matrix metalloproteinase-2-deficient mice. Investigative ophthalmology & visual science 2003, 44:403-8.
[65] Ohno-Matsui K, Uetama T, Yoshida T, Hayano M, Itoh T, Morita I, Mochizuki M: Reduced retinal angiogenesis in MMP-2-deficient mice. Investigative ophthalmology & visual science 2003, 44:5370-5.
[66] Cai J, Yin G, Lin B, Wang X, Liu X, Chen X, Yan D, Shan G, Qu J, Wu S: Roles of NFkappaB-miR-29s-MMP-2 circuitry in experimental choroidal neovascularization. Journal of neuroinflammation 2014, 11:88.
[67] Van Lint P, Libert C: Chemokine and cytokine processing by matrix metalloproteinases and its effect on leukocyte migration and inflammation. Journal of leukocyte biology 2007, 82:1375-81.
[68] Vinores SA, Xiao WH, Aslam S, Shen J, Oshima Y, Nambu H, Liu H, Carmeliet P, Campochiaro PA: Implication of the hypoxia response element of the Vegf promoter in mouse models of retinal and choroidal neovascularization, but not retinal vascular development. Journal of cellular physiology 2006, 206:749-58.

[69] Aiello LP, Pierce EA, Foley ED, Takagi H, Chen H, Riddle L, Ferrara N, King GL, Smith LE: Suppression of retinal neovascularization in vivo by inhibition of vascular endothelial growth factor (VEGF) using soluble VEGF-receptor chimeric proteins. Proceedings of the National Academy of Sciences of the United States of America 1995, 92:10457-61.
[70] Okamoto N, Tobe T, Hackett SF, Ozaki H, Vinores MA, LaRochelle W, Zack DJ, Campochiaro PA: Transgenic mice with increased expression of vascular endothelial growth factor in the retina: a new model of intraretinal and subretinal neovascularization. The American journal of pathology 1997, 151:281-91.
[71] Kwak N, Okamoto N, Wood JM, Campochiaro PA: VEGF is major stimulator in model of choroidal neovascularization. Investigative ophthalmology & visual science 2000, 41:3158-64.
[72] Aderka D: The potential biological and clinical significance of the soluble tumor necrosis factor receptors. Cytokine & growth factor reviews 1996, 7:231-40.
[73] Fessler SP, Chin YR, Horwitz MS: Inhibition of tumor necrosis factor (TNF) signal transduction by the adenovirus group C RID complex involves downregulation of surface levels of TNF receptor 1. Journal of virology 2004, 78:13113-21.
[74] Cook EB, Stahl JL, Graziano FM, Barney NP: Regulation of the receptor for TNFalpha, TNFR1, in human conjunctival epithelial cells. Investigative ophthalmology & visual science 2008, 49:3992-8.
[75] Xanthoulea S, Pasparakis M, Kousteni S, Brakebusch C, Wallach D, Bauer J, Lassmann H, Kollias G: Tumor necrosis factor (TNF) receptor shedding controls thresholds of innate immune activation that balance opposing TNF functions in infectious and inflammatory diseases. The Journal of experimental medicine 2004, 200:367-76.
[76] D'Andrea A, Aste-Amezaga M, Valiante NM, Ma X, Kubin M, Trinchieri G: Interleukin 10 (IL-10) inhibits human lymphocyte interferon gamma-production by suppressing natural killer cell stimulatory factor/IL-12 synthesis in accessory cells. The Journal of experimental medicine 1993, 178:1041-8.
[77] Matsumura N, Kamei M, Tsujikawa M, Suzuki M, Xie P, Nishida K: Low-dose lipopolysaccharide pretreatment suppresses choroidal neovascularization via IL-10 induction. PloS one 2012, 7:e39890.
[78] te Velde AA, Huijbens RJ, Heije K, de Vries JE, Figdor CG: Interleukin-4 (IL-4) inhibits secretion of IL-1 beta, tumor necrosis factor alpha, and IL-6 by human monocytes. Blood 1990, 76:1392-7.
[79] Mijatovic T, Kruys V, Caput D, Defrance P, Huez G: Interleukin-4 and -13 inhibit tumor necrosis factor-alpha mRNA translational activation in lipopolysaccharide-induced mouse macrophages. The Journal of biological chemistry 1997, 272:14394-8.
[80] Gautam S, Tebo JM, Hamilton TA: IL-4 suppresses cytokine gene expression induced by IFN-gamma and/or IL-2 in murine peritoneal macrophages. Journal of immunology 1992, 148:1725-30.
[81] Kondo T, Vicent D, Suzuma K, Yanagisawa M, King GL, Holzenberger M, Kahn CR: Knockout of insulin and IGF-1 receptors on vascular endothelial cells protects against retinal neovascularization. The Journal of clinical investigation 2003, 111:1835-42.
[82] Lu M, Amano S, Miyamoto K, Garland R, Keough K, Qin W, Adamis AP: Insulin-induced vascular endothelial growth factor expression in retina. Investigative ophthalmology & visual science 1999, 40:3281-6.
[83] Poulaki V, Qin W, Joussen AM, Hurlbut P, Wiegand SJ, Rudge J, Yancopoulos GD, Adamis AP: Acute intensive insulin therapy exacerbates diabetic blood-retinal barrier breakdown via hypoxia-inducible factor-1alpha and VEGF. The Journal of clinical investigation 2002, 109:805-15.
[84] Frystyk J, Grofte T, Skjaerbaek C, Orskov H: The effect of oral glucose on serum free insulin-like growth factor-I and -II in health adults. The Journal of clinical endocrinology and metabolism 1997, 82:3124-7.
[85] Delafontaine P, Song YH, Li Y: Expression, regulation, and function of IGF-1, IGF-1R, and IGF-1 binding proteins in blood vessels. Arteriosclerosis, thrombosis, and vascular biology 2004, 24:435-44.

[86] Bach LA: Recent insights into the actions of IGFBP-6. Journal of cell communication and signaling 2015, 9:189-200.
[87] Liu B, Lee KW, Anzo M, Zhang B, Zi X, Tao Y, Shiry L, Pollak M, Lin S, Cohen P: Insulin-like growth factor-binding protein-3 inhibition of prostate cancer growth involves suppression of angiogenesis. Oncogene 2007, 26:1811-9.
[88] Rho SB, Dong SM, Kang S, Seo SS, Yoo CW, Lee DO, Woo JS, Park SY: Insulin-like growth factor-binding protein-5 (IGFBP-5) acts as a tumor suppressor by inhibiting angiogenesis. Carcinogenesis 2008, 29:2106-11.
[89] Zhang C, Lu L, Li Y, Wang X, Zhou J, Liu Y, Fu P, Gallicchio MA, Bach LA, Duan C: IGF binding protein-6 expression in vascular endothelial cells is induced by hypoxia and plays a negative role in tumor angiogenesis. International journal of cancer 2012, 130:2003-12.
[90] Eubank TD, Galloway M, Montague CM, Waldman WJ, Marsh CB: M-CSF induces vascular endothelial growth factor production and angiogenic activity from human monocytes. Journal of immunology 2003, 171:2637-43.
[91] Priceman SJ, Sung JL, Shaposhnik Z, Burton JB, Torres-Collado AX, Moughon DL, Johnson M, Lusis AJ, Cohen DA, Iruela-Arispe ML, Wu L: Targeting distinct tumor-infiltrating myeloid cells by inhibiting CSF-1 receptor: combating tumor evasion of antiangiogenic therapy. Blood 2010, 115:1461-71.
[92] Schubert SY, Benarroch A, Ostvang J, Edelman ER: Regulation of endothelial cell proliferation by primary monocytes. Arteriosclerosis, thrombosis, and vascular biology 2008, 28:97-104.
[93] Arnold T, Betsholtz C: The importance of microglia in the development of the vasculature in the central nervous system. Vascular cell 2013, 5:4.
[94] Apte RS, Richter J, Herndon J, Ferguson TA: Macrophages inhibit neovascularization in a murine model of age-related macular degeneration. PLoS medicine 2006, 3:e310.
[95] Hasegawa E, Oshima Y, Takeda A, Saeki K, Yoshida H, Sonoda KH, Ishibashi T: IL-27 inhibits pathophysiological intraocular neovascularization due to laser burn. Journal of leukocyte biology 2012, 91:267-73.
[96] Liu J, Copland DA, Horie S, Wu WK, Chen M, Xu Y, Paul Morgan B, Mack M, Xu H, Nicholson LB, Dick AD: Myeloid cells expressing VEGF and arginase-1 following uptake of damaged retinal pigment epithelium suggests potential mechanism that drives the onset of choroidal angiogenesis in mice. PloS one 2013, 8:e72935.
[97] Grossniklaus HE, Ling JX, Wallace TM, Dithmar S, Lawson DH, Cohen C, Elner VM, Elner SG, Sternberg P, Jr.: Macrophage and retinal pigment epithelium expression of angiogenic cytokines in choroidal neovascularization. Molecular vision 2002, 8:119-26.

Figure legends

Figure 1. Effect of colony stimulating factor-1 receptor (CSF-1R) inhibition on choroidal neovascularization. A: Experimental setup. **B:** Representative autofluorescence images of a MacGreen mouse retina before (PLX5622 d-7, n = 3 mice) and 7 days after the start of PLX5622 diet (PLX5622 d0, n = 3). GFP positive microglia cells are drastically diminished in the retina after 7 days of PLX5622 diet. **C:** Representative fluorescein angiographs of choroidal neovascularization (CNV)-subjected eyes at different time points in control or PLX5622-fed mice. **D:** CNV area measurements in fluorescein angiographs of control or PLX5622-fed mice. CNV area was gradually decreased in control (CNV) and PLX5622-fed mice. ***$P < 0.001$, repeated measures one way ANOVA followed by Tukey's post hoc analysis; n ≥ 14 eyes per group. Statistically significant reduction of the lesion size was observed in the presence of PLX5622 at day 14 compared to the control. ***$P < 0.001$, ordinary one way ANOVA followed by Tukey's post hoc analysis; n ≥ 14 eyes per group. Individual CNV lesions are plotted in the graph.

Figure 2. *Ex vivo* evaluation of microglia and accumulation of monocyte-derived macrophages in the laser site. A: Isolectin and Iba-1 staining in the choroid-RPE whole mounts and Iba-1 staining in retinal whole mounts 14 days post choroidal neovascularization (CNV) in control (n ≥ 6 mice per group) and PLX5622-fed mice. Iba-1–positive cells accumulate at the laser site in the choroid-RPE and in the retina of control CNV-subjected mice. In PLX5622-fed mice Iba-1–positive cells are detected in the choroid-RPE but not in the retinal whole mounts. The numbers indicate the three different laser spots and the asterisks indicate the optic nerve head. Scale bars: 500 μm; magnification: 10x **B:** Higher magnification of Iba-1 staining in control-fed mice subjected to CNV, 14 days after the laser

application. In the choroid-RPE and the outer retina, Iba-1–positive cells accumulated around the laser site and their morphology is characterized by increased soma size and retracted processes. In the inner retina a ramified morphology is observed. Scale bars: 200 μm; magnification: 40x. **C:** Representative photomicrographs of Iba-1–positive cells in retinal sections of control ($n \geq 3$ mice per time point) or PLX5622-fed ($n \geq 3$ mice per time point) CNV-subjected mice. Iba-1–positive cells accumulated in the outer retinal and the choroid-RPE in the CNV eyes (first and second panel). In mice fed with PLX5622, Iba-1–positive cells also accumulated in the outer retina and choroid-RPE; however, they were fewer in number and were almost absent 7 days after CNV (third and fourth panel). IPL, inner plexiform layer; ONL, outer nuclear layer. Scale bars: 200 μm; magnification: 20x. **D:** Representative photomicrographs of Iba-1 and CSF-1R-GFP positive cells in retinal sections of control or PLX5622-fed mice 14 days after CNV ($n \geq 3$ mice per treatment). Most of the CSF-1R-GFP positive cells are co-localized with Iba-1 while a few of them are Iba-1 negative (arrows). Scale bars: 100 μm; magnification: 40x.

Figure 3. Flow cytometry analysis of microglia/macrophages population in the retina of choroidal neovascularization (CNV)-subjected mice. **A:** Representative flow cytometry plots at different time points post CNV in control and PLX5622-fed animals. Microglia were identified as $CD45^{low}$ $CD11b^{+}$ and macrophages as $CD45^{hi}$ $CD11b^{+}$. **B:** Quantification of microglia (upper panel; $CD45^{low}$ $CD11b^{+}$) and macrophages (lower panel; $CD45^{hi}$ $CD11b^{+}$) in the retina, 3 and 7 days post CNV, in the presence or absence of PLX5622. Elevated number of microglia and macrophages is observed 3 and 7 days post CNV ($n \geq 5$ mice per group). PLX5622 reduces the number of microglia and macrophages in the retina ($n \geq 5$ mice per group). **C:** Quantification of $CSF\text{-}1R^{+}$ or $MHC\text{-}II^{+}$ microglia (first and second graph) and $CSF\text{-}1R^{+}$ or $MHC\text{-}II^{+}$ macrophages (third and fourth graph), expressed as a percentage of the

total number of microglia or macrophages, respectively. No statistically significant difference was observed in the number of CSF-1R^{+} microglia and macrophages in the presence or absence of PLX5622. MHC-II^{+} microglia and macrophages were detected in the retina at the early course of CNV (day 3), yet this increase was not statistically significant compared to the naïve tissue. PLX5622 reduces the expression of MHC-II by these cells ***$P < 0.001$, one-way ANOVA followed by Tukey's post hoc analysis or Kruskal-Wallis test followed by Dunn`s multiple comparison test, $n \geq 5$ per group).

Figure 4. Quantification of immune cell population in the choroid-RPE using flow cytometry analysis. **A:** The numbers of CD11c^{+} cells (first graph) in the choroid-RPE is elevated 3 days after choroidal neovascularization (CNV) and returns to control levels at day 7 post CNV. PLX5622 reduces CD11c^{+} cell numbers below control levels. Leukocyte numbers (second graph) peak at day 3 after CNV and their numbers are reduced in the presence of PLX5622. A slight increase in neutrophil numbers is detected 3 days post CNV (third graph). **B:** Leukocytes were further gated based on the expression of Ly6G and Ly6C. Ly6G^{neg} Ly6C$^{low/neg}$ SSC-H^{low} cells are reduced in the presence of PLX5622 while no differences are observed between the naïve and CNV subjected tissues (first graph). On the other hand, Ly6G^{neg} Ly6C^{hi} inflammatory monocytes/macrophages are increased 3 days post CNV and decreased thereafter (second graph) and this phenomenon is prevented by PLX5622. **C:** No difference is observed in the expression of colony stimulating factor-1 receptor (CSF-1R) by Ly6G^{neg} Ly6C$^{low/neg}$ SSC-H^{low} (first graph) or Ly6G^{neg} Ly6C^{hi} monocytes/macrophages (second graph) between different treatments. *$P < 0.05$, **$P < 0.01$, ***$P < 0.001$, ordinary one way ANOVA with Tukey's post hoc analysis or Kruskal-Wallis test followed by Dunn`s multiple comparison test; $n \geq 5$ for each treatment.

Table 1. Effect of laser-induced CNV on cytokine/chemokine levels in the C57BL/6J mouse eyecups in the presence or absence of PLX5622.

	Day 3		Day 7	
Factors	**CNV**	**CNV+PLX5622**	**CNV**	**CNV+PLX5622**
Chemokines				
CCL3	1.60*	1.11	0.85‡‡	0.55
CCL9	1.58***	2.36***†††	1.26	2.62***†††
CX3CL1	1.34	4.59***	1.39	3.75***
CXCL2	1.19	1.46***	1.08	1.39**†
CXCL13	1.34	2.12***†	1.06	1.46
CXCL16	1.29	2.38***†††	1.11	2.45***†††
Growth factors				
bFGF	1.67	2.06*	2.12***	3.00***†
IGFBP-3	1.33**	1.83***†††	1.08	1.70***†††
IGFBP-5	1.45*	2.41***†††	1.12	1.92***†††
IGFBP-6	1.13	2.80**†	1.32	1.84
GM-CSF	1.68*	2.89***†††	1.66*	1.91**‡‡
M-CSF	1.12	1.33*	1.15	1.02
TNF superfamily				
CD30	1.21	2.03**†	1.09	1.54
CD30 L	1.43*	1.40	1.09	0.92

Fas ligand	0.79	1.75††	0.85	0.93
sTNFRI	1.53*	2.58***†††	0.86‡‡	2.35***†††
Pro-Inflammatory cytokines				
IFN-g	1.70*	0.54†††	1.14‡	0.46†
IL-1α	1.34*	2.31***†††	1.12	1.60***††‡‡‡
IL-12 p70	1.48**	1.76***	1.09‡	1.50*
TCA-3	1.20	1.86***†††	0.95	1.73***†††
TIMP-1α	1.23	1.59**	0.93	1.41†
Anti-inflammatory cytokines				
IL-4	1.06	2.72†††	0.89	2.75†††
IL-10	1.40	3.13***†††	1.53	2.00*‡
IL-13	1.45**	1.35	1.08†	0.84‡
Tissue remodeling				
MMP-2	1.86***	5.07***†††	0.84‡	5.62***†††
MMP-3	1.59*	1.85**	1.13	2.29***†††
Fc-gamma receptors				
Fc gamma RIIB	2.19**	0.43††	1.45	0.89
Adhesion molecules				
VCAM-1	1.54**	2.84***†††	1.57***	3.47***†††

Semi-quantitative analysis of inflammatory mediators' protein levels in the retina-choroid-RPE complex, 3 and 7 days after CNV, in the presence or absence of PLX5622. All data are normalized to naive tissues.

$^{*}P < 0.05$, $^{**}P < 0.01$, $^{***}P < 0.001$ compared to naïve.

†$P < 0.05$, ††$P < 0.01$, †††$P < 0.001$ compared to CNV.

‡$P < 0.05$, ‡‡$P < 0.01$, ‡‡‡$P < 0.001$ compared to the same treatment at day 3.

Only targets with statistically significant differences are shown in the table. Targets that were examined but did not show statistically significant differences included IL-6, TNFα, VEGF, MCP-1, G-CSF, and CCL5 among others.

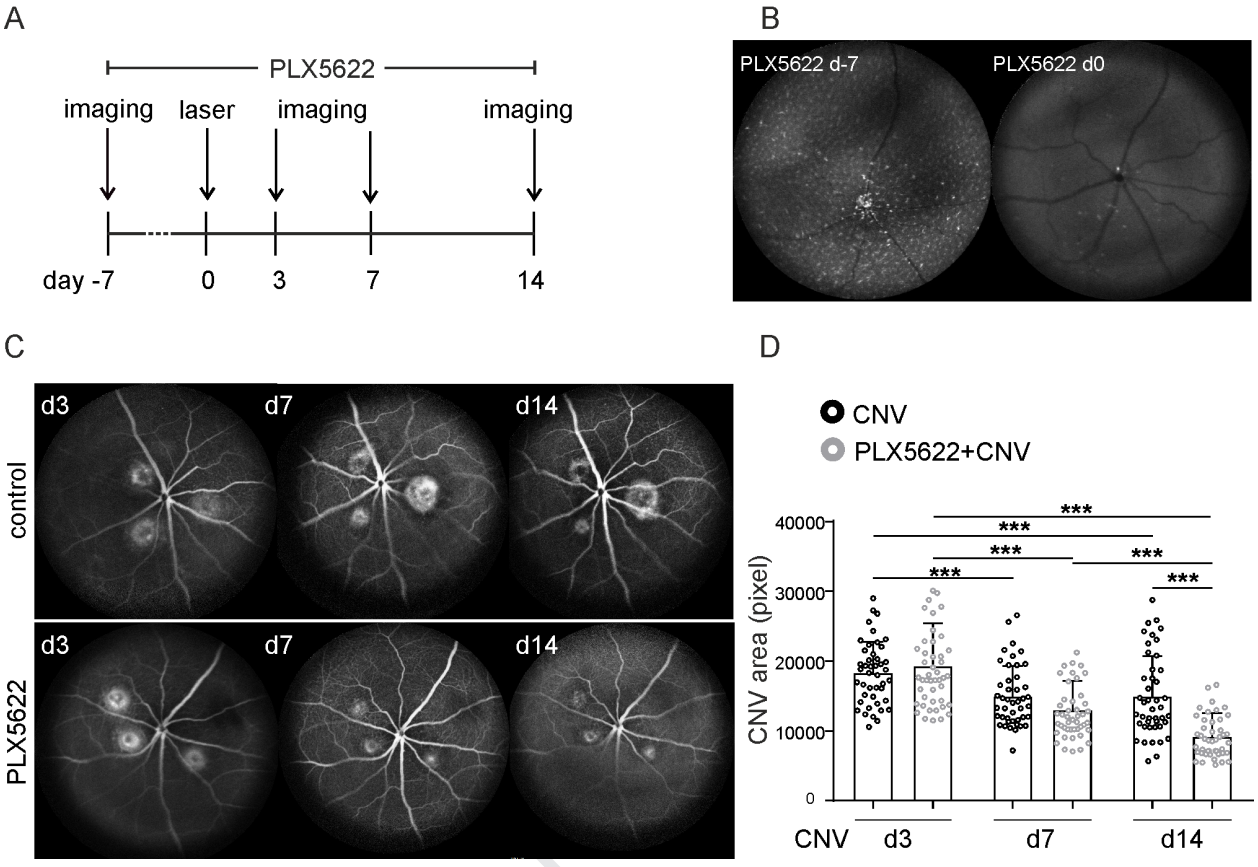
A
PLX5622
imaging
laser
imaging
imaging
day -7
0
3
7
14
B
PLX5622 d-7
PLX5622 d0
C
control
PLX5622
d3
d7
d14
d3
d7
d14
D
CNV
PLX5622+CNV
CNV area (pixel)
40000
30000
20000
10000
0
***
***
***
***
***
***
CNV
d3
d7
d14

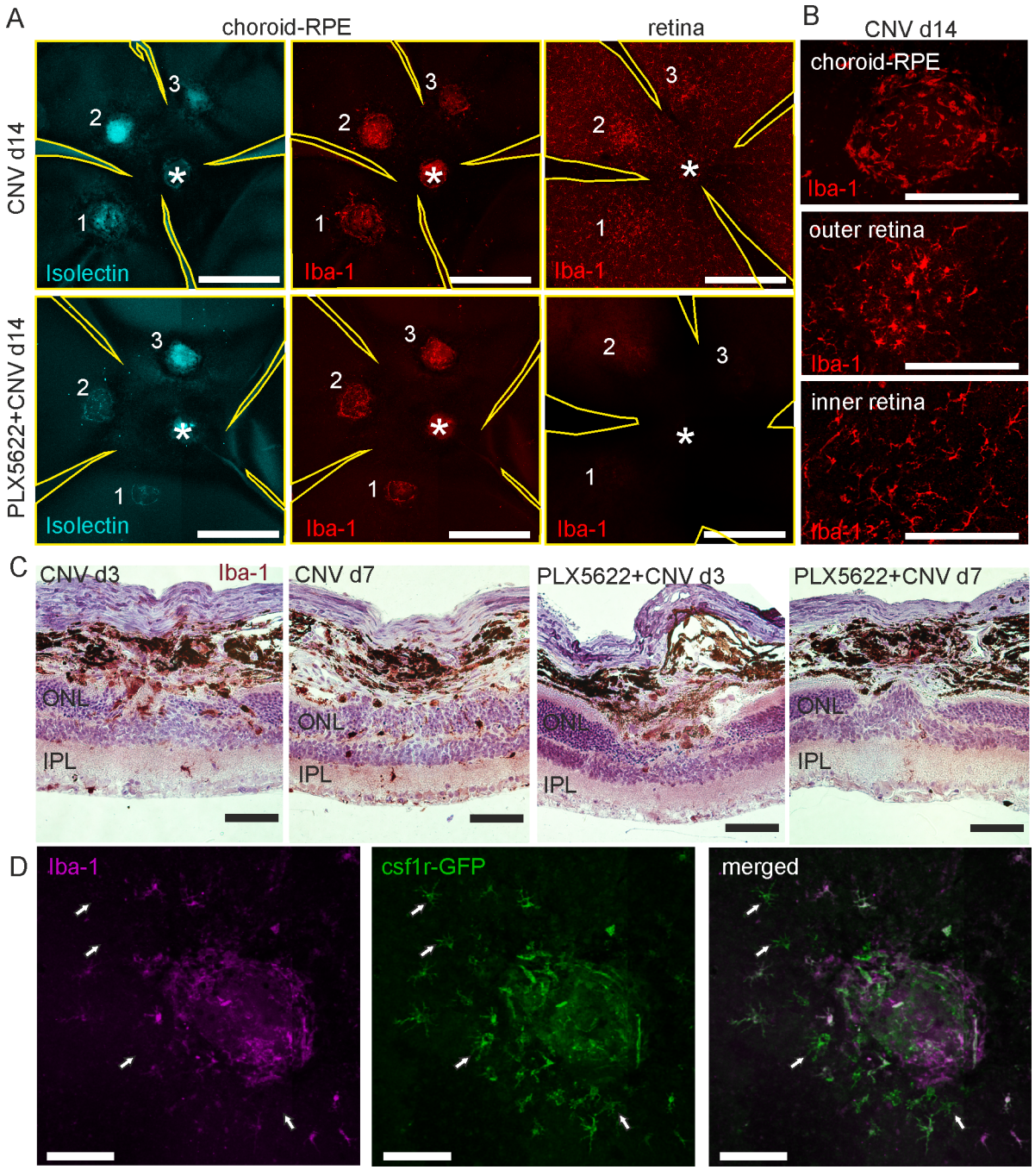
A
choroid-RPE
retina
CNV d14
PLX5622+CNV d14
Isolectin
Iba-1
B
CNV d14
choroid-RPE
outer retina
inner retina
C
CNV d3
CNV d7
PLX5622+CNV d3
PLX5622+CNV d7
ONL
IPL
D
Iba-1
csf1r-GFP
merged

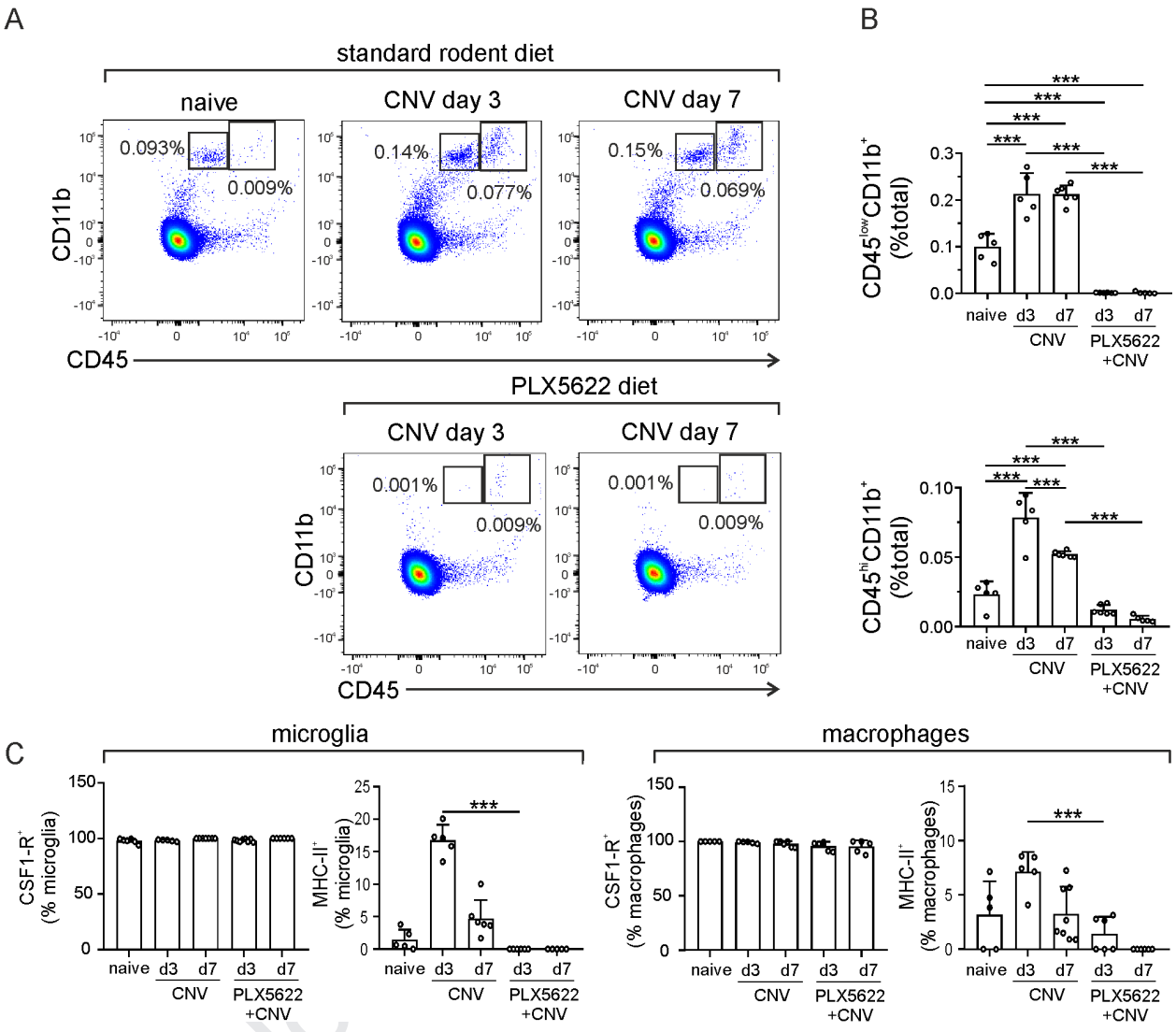
A
standard rodent diet
naive
CNV day 3
CNV day 7
0.093%
0.009%
0.14%
0.077%
0.15%
0.069%
CD11b
CD45
PLX5622 diet
CNV day 3
CNV day 7
0.001%
0.009%
0.001%
0.009%
CD11b
CD45
B
CD45low CD11b+ (%total)
CD45hi CD11b+ (%total)
naive
d3
d7
CNV
PLX5622 +CNV
C
microglia
macrophages
CSF1-R+ (% microglia)
MHC-II+ (% microglia)
CSF1-R+ (% macrophages)
MHC-II+ (% macrophages)
***

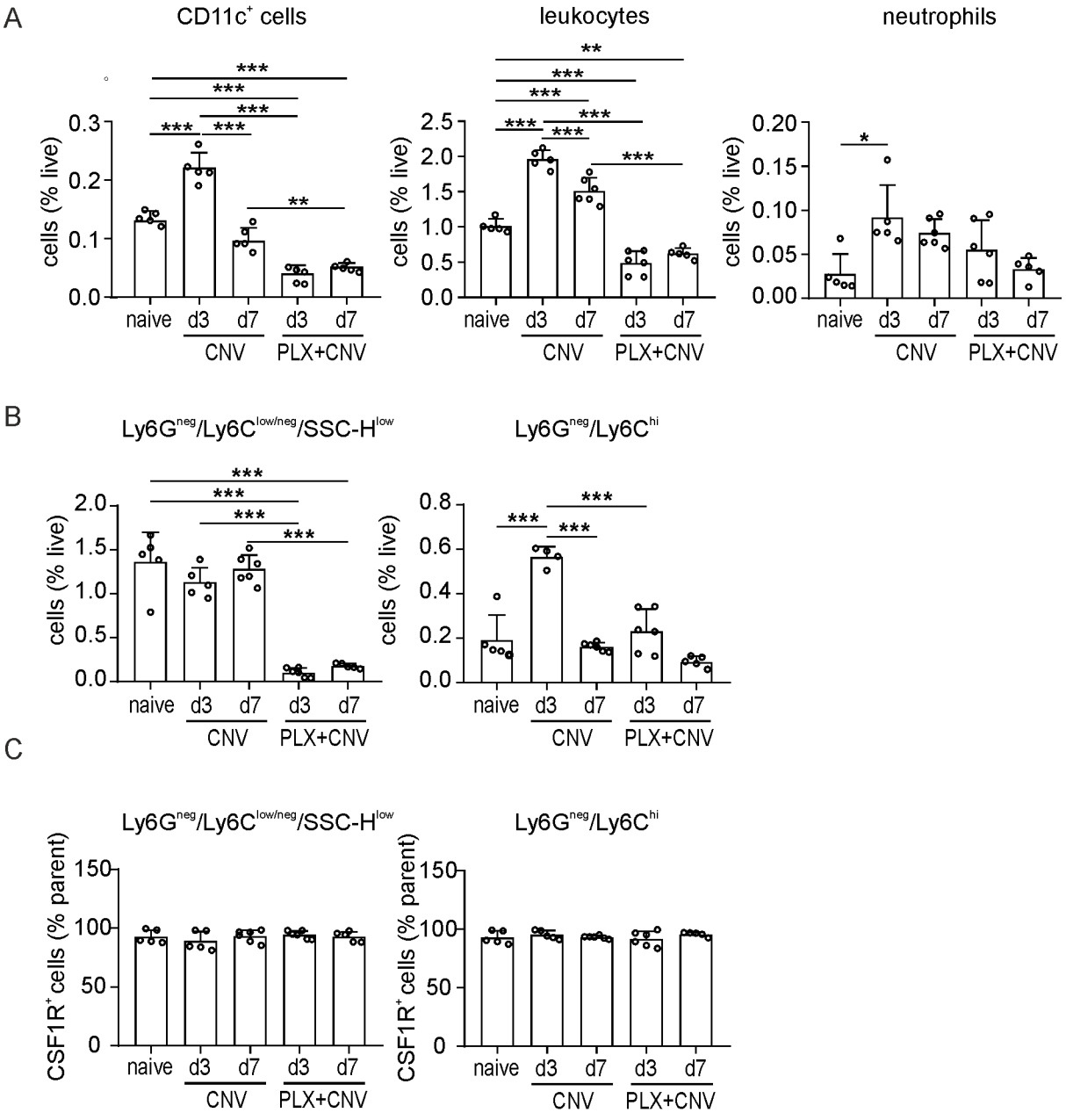
A
CD11c+ cells
leukocytes
neutrophils
cells (% live)
naive
d3
d7
d3
d7
CNV
PLX+CNV
B
Ly6Gneg/Ly6Clow/neg/SSC-Hlow
Ly6Gneg/Ly6Chi
C
CSF1R+cells (% parent)